

# Fabrication of Fe<sub>3</sub>O<sub>4</sub>-L-dopa-Cu<sup>II</sup>/Sn<sup>IV</sup>@Micro-Mesoporous-SiO<sub>2</sub> Catalyst Applied to Baeyer–Villiger Oxidation Reaction

Hongfei Huo, Li Wu, Jianxin Ma, Honglei Yang, Le Zhang, Yuanyuan Yang, Shuwen Li, and Rong Li\*<sup>[a]</sup>

A Magnetic mFe<sub>3</sub>O<sub>4</sub>-L-dopa-Cu<sup>II</sup>/Sn<sup>IV</sup>@micro-mesoporous-SiO<sub>2</sub> catalyst was successfully prepared. The catalyst exhibits high and stable catalytic activity for the Baeyer–Villiger oxidation reaction with air as oxidant. Furthermore, the selectivity can reach nearly 100%. Meanwhile the catalyst can be easily sepa-

rated by an external magnet and reused at least up to five cycles without any notable loss in catalytic activity. In addition, the effect of Sn and Cu on the oxidation of cyclohexanone is discussed.

## 1. Introduction

Lactones have been applied widely as key molecules for the synthesis of important bioactive compounds, natural products and polymers; and represent a valuable family of synthons for various organic transformations. Lactones or esters can be synthesized from their corresponding ketones by employing the Baeyer–Villiger (B-V) oxidation.<sup>[1–3]</sup> The B-V oxidation is one of the most significant and practical oxidation reactions and has been extensively used for the synthesis of antibiotics, steroids, pheromones, monomers for polymerization, and various fine chemicals.<sup>[4–6]</sup> In general, B-V oxidations have usually been conducted by highly expensive, hazardous, shock sensitive, and environmentally malignant organic peracids as oxidants,<sup>[5]</sup> therefore, developing greener alternatives as oxidants for B-V reaction is a technologically crucial issue. According to many reports, two main protocols have been used for investigating greener oxidants for the B-V reaction.<sup>[7]</sup> One is the use of aqueous hydrogen peroxide as oxidant,<sup>[4,8–11]</sup> this, however carries some shortcomings. For example, hydrogen peroxide is kinetically inert compared to peracids and the presence of water in the reaction mixture leads to the hydrolysis of the product.<sup>[12]</sup> Moreover, it is dangerous to use high concentrations of hydrogen peroxide in organic solvents.<sup>[12]</sup> The other important protocol has been demonstrated in the presence of aldehydes as a sacrificing agent, which is known as the Mukaiyama method.<sup>[13]</sup> There are some reports in which heterogeneous catalysts have been developed for effective B-V oxidation with peracids and H<sub>2</sub>O<sub>2</sub>.<sup>[10,14,15]</sup>

Research on B-V oxidation using molecular oxygen, benzaldehyde and a heterogeneous catalyst are rare.<sup>[1,23,7]</sup> The O<sub>2</sub>/al-

dehyde oxidation system is fascinating, because it has the potential to lower the cost of current industrial processes<sup>[1]</sup> and avoid using organic peracids. Nevertheless, O<sub>2</sub>/aldehyde systems typically require pure oxygen and large amounts of sacrificing agents over the stoichiometric ratio (e.g., 3 equiv). If pure oxygen can be replaced with air and the amounts of sacrificing agents over the stoichiometric ratio can be lower, the system will become more fascinating and environmentally friendly. Recently, B-V oxidation reaction has been reported to be catalyzed by different catalysts (graphite, carbon materials, *m*-ZrP) with no more than 2 molar equiv of benzaldehyde as sacrificial agents. However, these systems suffered from the limitations of much consumption of metal, relatively low activity or longer reaction time.<sup>[1,3,8]</sup>

Previous studies showed that Sn as Lewis acid centers incorporated into a zeolite framework (zeolite Beta) have been found to be very active and highly selective catalysts for the B-V oxidation of ketones with hydrogen peroxide.<sup>[16,17]</sup> For instance, tin-containing beta zeolite could oxidize adamantanone and cyclohexanone to the corresponding lactones with excellent selectivity, which was developed by Corma et al.<sup>[17]</sup> In addition, introducing Sn into the siliceous framework of mesoporous molecular sieves of different structural types resulted in the formation of highly active and selective catalysts for oxidative reactions.<sup>[18]</sup>

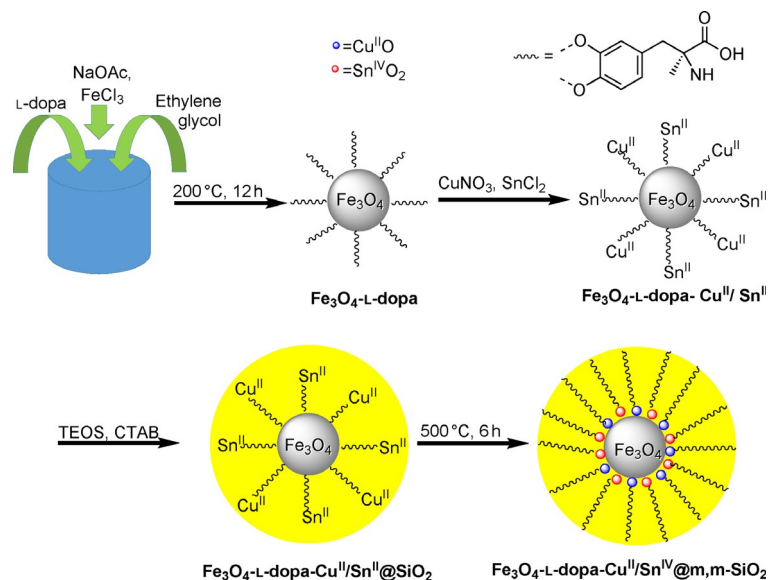
Copper is a fascinating metal catalyst especially for the oxidation reactions such as B-V oxidation, benzylic oxidation, aldehydes to acids, C–H oxidation, reaction of carbanions and carbanion equivalents and alkene oxidation etc.<sup>[19–25]</sup> Inspired by the efficiency of tin-containing zeolite and Cu<sup>II</sup> in oxidation reactions, we envisaged that the efficiency in the B-V oxidations of ketones could be improved by Cu<sup>II</sup> and SnO<sub>2</sub> bimetallic catalysts.

Herein, the aerobic B-V oxidation of ketones catalyzed by Cu<sup>II</sup> and Sn<sup>IV</sup> using Fe<sub>3</sub>O<sub>4</sub>-L-dopa-Cu<sup>II</sup>/Sn<sup>IV</sup>@m,m-SiO<sub>2</sub> catalyst was developed. The fabrication procedure involves six main

[a] H. Huo, L. Wu, J. Ma, H. Yang, L. Zhang, Y. Yang, S. Li, Prof. Dr. R. Li  
College of Chemistry and Chemical Engineering  
Lanzhou University  
Tianshui South Road, Lanzhou, 730000 (P.R. China)  
E-mail: liyirong@lzu.edu.cn

Supporting Information for this article is available on the WWW under <http://dx.doi.org/10.1002/cctc.201501107>.

steps as shown in Scheme 1. The role of bimetallic catalysts in the aerobic oxidation was discussed and a bimetallic mechanism involving activated cyclohexanone for enhancing the efficiency was also proposed. The present study provides an example that the bimetallic catalyst could catalyze the reaction of the B-V oxidation of cyclohexanone actively.



Scheme 1. Preparation of the catalysts.

## 2. Experimental

### 2.1. Synthesis of the L-dopa modified magnetic nanoparticles<sup>[26]</sup>

Typically,  $\text{FeCl}_3$  (0.973 g) was dissolved in ethylene glycol (30 mL) to form a clear solution, followed by the addition of NaOAc (1.970 g) and L-dopa (0.0547 g). The mixture was stirred vigorously for 30 min, and then sealed in a Teflon-lined stainless-steel autoclave (50 mL capacity). Then, the autoclave was heated to and maintained at 200 °C for 12 h, and allowed to cool to room temperature. The black products were separated by magnetic force and washed several times with ethanol and dried at 50 °C for 24 h.

### 2.2. Loading of $\text{Sn}^{\text{II}}$ and $\text{Cu}^{\text{II}}$ on L-dopa functionalized magnetic nanoparticles ( $\text{Fe}_3\text{O}_4\text{-L-dopa-Cu}^{\text{II}}/\text{Sn}^{\text{II}}$ )

$\text{Fe}_3\text{O}_4\text{-L-dopa}$  (300 mg) was dispersed in distilled water (120 mL) and stirred for 20 min as part A.  $\text{SnCl}_2 \cdot 2\text{H}_2\text{O}$  (0.112 g) and  $\text{Cu}(\text{NO}_3)_2 \cdot 3\text{H}_2\text{O}$  (0.120 g) was dissolved in HCl solution (25 mL 0.02 M) as part B. Parts A and B were mixed together under ultrasonication for 1 h. Subsequently, the mixture was stirred vigorously for 8 h. At last, the precipitate was separated by magnetic force, washed three times with distilled water, and then dried at 50 °C for 12 h.

### 2.3. Production of $\text{Fe}_3\text{O}_4\text{-L-dopa-Cu}^{\text{II}}/\text{Sn}^{\text{IV}}@\text{m,m-SiO}_2$

To grow a mesoporous silica shell on the  $\text{Fe}_3\text{O}_4\text{-L-dopa-Cu}^{\text{II}}/\text{Sn}^{\text{II}}$  microspheres, the as-made  $\text{Fe}_3\text{O}_4\text{-L-dopa-Cu}^{\text{II}}/\text{Sn}^{\text{II}}$  nanospheres (300 mg) are redispersed in a mixed solution containing CTAB (0.45 g, 1.2 mmol), distilled water (100 mL), concentrated ammonia solution (2.0 mL, 28 wt %), and ethanol (150 mL). The resultant mixed solution is ultrasonic dispersed for 5 min and then stirred for 30 min to form a uniform dispersion. Subsequently, TEOS (0.8 mL) is added drop-wise to the dispersion under continuous stirring. After magnetic stirring for 6 h, the product is collected by centrifugation (8000 rpm, 3 min) and washed with distilled water and ethanol for several times. Then the collected nanospheres are dried at 40 °C in a vacuum drying oven overnight for further use. Finally, the product was calcined at 500 °C (ramping rate, 3 °C min<sup>-1</sup>) in air atmosphere for 6 h to remove CTAB template and other organic species. The amount of Cu, Sn, and Fe in the  $\text{Fe}_3\text{O}_4\text{-L-dopa-Cu}^{\text{II}}/\text{Sn}^{\text{IV}}@\text{m,m-SiO}_2$  catalysts was found to be 1.0, 4.0, and 14 wt %, based on ICP analysis.  $\text{Fe}_3\text{O}_4\text{-L-dopa-Cu}^{\text{II}}/\text{Sn}^{\text{IV}}@\text{m,m-SiO}_2$  has coated the  $\text{CuO}$  and  $\text{SnO}_2$  particles, prevented aggregation of metallic nanoparticles, promoted the mass diffusion and transported of reactants.

### 2.4. Characterization of the catalyst

The synthesized catalyst was confirmed by corresponding characterization means. The morphology and microstructure of the catalyst were characterized by transmission electron microscopy (TEM). The TEM and EDX images were obtained through Tecnai G2 F30 electron microscope operating at 300 kV, and samples were obtained by placing a drop of a colloidal solution onto a nickel grid and evaporating the solvent in air at room temperature. The conversion was estimated by GC (P.E. AutoSystem XL) or GC-MS (Agilent 6,890N/5,973N). Inductive coupled plasma atomic emission spectrometer (ICP-AES) analysis was conducted with PerkinElmer (Optima-4300DV). Specific surface areas were calculated by the Brunauer–Emmett–Teller (BET) method and pore sizes by the hybrid density functional theory cylindrical pores in pillared clay model non-negative regularization method (Tristar II 3020). Inductive coupled plasma atomic emission spectrometer (ICPAES) analysis was conducted with PerkinElmer (Optima-4300DV). Magnetic measurement of  $\text{Fe}_3\text{O}_4$  and  $\text{Fe}_3\text{O}_4\text{-L-dopa-Cu}^{\text{II}}/\text{Sn}^{\text{IV}}@\text{m,m-SiO}_2$  was performed using a Quantum Design vibrating sample magnetometer (VSM) at room temperature in an applied magnetic field sweep from –15 to 15 kOe.

### 2.5. Catalytic activity and recyclability

The B-V oxidation of cyclohexanone was performed in a three-neck bottle placed in a temperature-controlled water bath. Typically, dichloroethane (DCE, 10 mL), a certain amount of cyclohexanone, benzaldehyde and  $\text{Fe}_3\text{O}_4\text{-L-dopa-Cu}^{\text{II}}/\text{Sn}^{\text{IV}}@\text{m,m-SiO}_2$  catalyst (50 mg) were charged into the flask. The mixture was stirred uniformly throughout the liquid. Air (20 mL min<sup>-1</sup>) was continuously introduced into the bottle. Then, the catalyst was collected by centrifugation washed with distilled water and ethanol for several times and calcined in air at 500 °C for 6 h before being subjected to the next catalytic cycle. The reaction system was analyzed by GC (P.E. AutoSystem XL) or GC-MS (Agilent 6,890N/5, 973N).

### 3.0 Results and discussion

#### 3.1. Characterizations of the $\text{Fe}_3\text{O}_4\text{-L-dopa-Cu}^{\text{II}}/\text{Sn}^{\text{IV}}@m,m\text{-SiO}_2$ catalyst

The morphologies and structures of the products at different synthetic steps are observed by TEM. Figure 1a shows the TEM image of  $\text{Fe}_3\text{O}_4$  nanospheres, in which well-dispersed particles with average diameter about 300 nm could be observed clearly. Figure 1b is an enlarged TEM image of  $\text{Fe}_3\text{O}_4$  nanospheres.

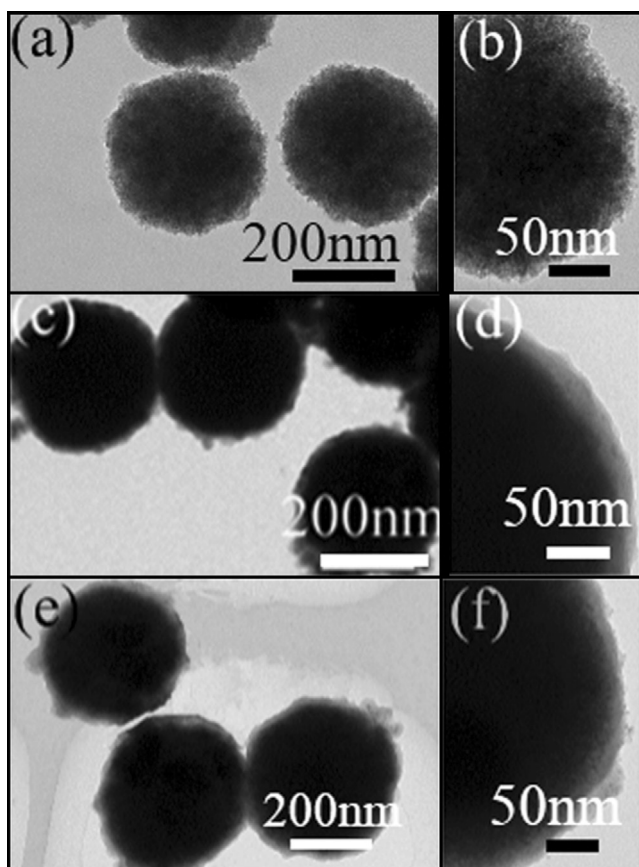


**Figure 1.** a) TEM of  $\text{Fe}_3\text{O}_4$  nanospheres; b) enlarged TEM of  $\text{Fe}_3\text{O}_4$  nanospheres; c) TEM of  $\text{Fe}_3\text{O}_4\text{-L-dopa-Cu}^{\text{II}}/\text{Sn}^{\text{IV}}@m,m\text{-SiO}_2$ ; d) enlarged TEM of  $\text{Fe}_3\text{O}_4\text{-L-dopa-Cu}^{\text{II}}/\text{Sn}^{\text{IV}}@m,m\text{-SiO}_2$ ; e) TEM of  $\text{Fe}_3\text{O}_4\text{-L-dopa-Cu}^{\text{II}}/\text{Sn}^{\text{IV}}@m,m\text{-SiO}_2$ ; f) enlarged TEM of  $\text{Fe}_3\text{O}_4\text{-L-dopa-Cu}^{\text{II}}/\text{Sn}^{\text{IV}}@m,m\text{-SiO}_2$ .

Figure 1c is a TEM of  $\text{Fe}_3\text{O}_4\text{-L-dopa-Cu}^{\text{II}}/\text{Sn}^{\text{IV}}@m,m\text{-SiO}_2$ . As can be seen from the image, the average diameter of the as-synthesized spherical particles was about 330 nm and they were nearly monodisperse. As shown in Figure 1e, the morphologies and structures of  $\text{Fe}_3\text{O}_4\text{-L-dopa-Cu}^{\text{II}}/\text{Sn}^{\text{IV}}@m,m\text{-SiO}_2$  nanospheres remain after calcination at  $500^\circ\text{C}$  in air atmosphere for 6 h. Figure 1d and f are enlarged TEM image of  $\text{Fe}_3\text{O}_4\text{-L-dopa-Cu}^{\text{II}}/\text{Sn}^{\text{IV}}@m,m\text{-SiO}_2$  and  $\text{Fe}_3\text{O}_4\text{-L-dopa-Cu}^{\text{II}}/\text{Sn}^{\text{IV}}@m,m\text{-SiO}_2$ , and the thickness between the two red line of the  $m,m\text{-SiO}_2$  shell is about 15 nm.

The elemental composition of the  $\text{Fe}_3\text{O}_4\text{-L-dopa-Cu}^{\text{II}}/\text{Sn}^{\text{IV}}@m,m\text{-SiO}_2$  samples was determined by EDX analysis. The result shown in Figure 2 reveals that the as-prepared products

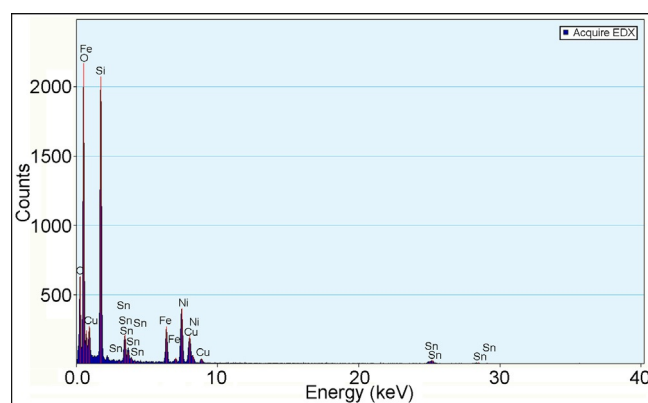


**Figure 2.** EDX spectrum of  $\text{Fe}_3\text{O}_4\text{-L-dopa-Cu}^{\text{II}}/\text{Sn}^{\text{IV}}@m,m\text{-SiO}_2$ .

contain Si, Cu, Sn, Fe, Ni, C, and O. Among these elements, Ni, C, and O are generally influenced by the nickel network support films and their degree of oxidation; Si, Cu, Sn, Fe, and O signals result from the products. The EDX results imply that the Cu and Sn nanoparticles have been successfully immobilized on the surface of  $\text{Fe}_3\text{O}_4$  nanoparticles. The content of Cu and Sn in the  $\text{Fe}_3\text{O}_4\text{-L-dopa-Cu}^{\text{II}}/\text{Sn}^{\text{IV}}@m,m\text{-SiO}_2$  catalysts was found to be 1.1 and 3.9 wt%, based on EDX analysis.

Shown in Figure 3 are representative nitrogen adsorption/desorption isotherms and the corresponding pore size distribution of the  $\text{Fe}_3\text{O}_4\text{-L-dopa-Cu}^{\text{II}}/\text{Sn}^{\text{IV}}@m,m\text{-SiO}_2$ . The BET surface area and single point total pore volume are  $765\text{ m}^2\text{g}^{-1}$  and  $0.45\text{ cm}^3\text{g}^{-1}$ , respectively, which are considerably large values.

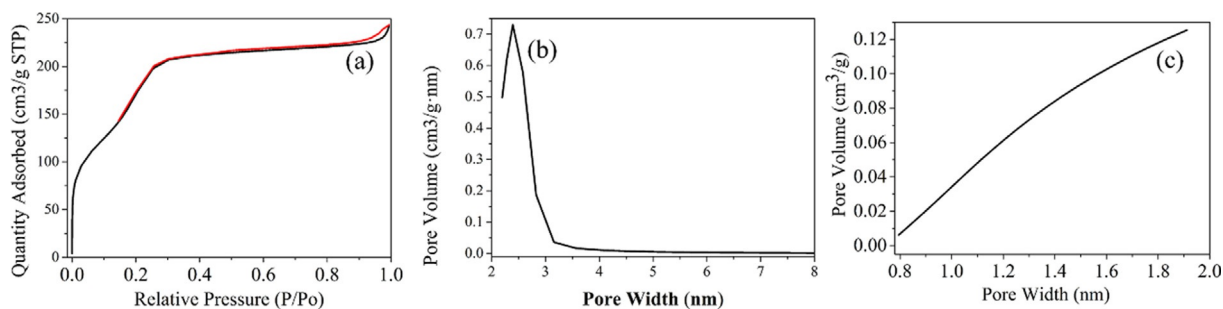


**Figure 3.** a) Nitrogen adsorption-desorption isotherm of the  $\text{Fe}_3\text{O}_4\text{-L-dopa-Cu}^{\text{II}}/\text{Sn}^{\text{IV}}@m,m\text{-SiO}_2$ , b) the corresponding mesoporous diameter distribution, and c) the corresponding micropore diameter distribution.

The pore size was calculated by using the non-negative regularization method, as shown in the inset of Figure 3b. As a result, average pore size was about 2.3 nm for  $\text{Fe}_3\text{O}_4\text{-L-dopa-Cu}^{\text{II}}/\text{Sn}^{\text{IV}}@m,m\text{-SiO}_2$ . On the basis of above analysis, it can be concluded that these data further identified the hollow mesoporous structure of the synthesized  $\text{Fe}_3\text{O}_4\text{-L-dopa-Cu}^{\text{II}}/\text{Sn}^{\text{IV}}@m,m\text{-SiO}_2$ .

Magnetization curves revealed the superparamagnetic behavior of the magnetic NPs. The hysteresis loops of  $\text{Fe}_3\text{O}_4$  and  $\text{Fe}_3\text{O}_4\text{-L-dopa-Cu}^{\text{II}}/\text{Sn}^{\text{IV}}@m,m\text{-SiO}_2$  are shown in Figure 4. It can

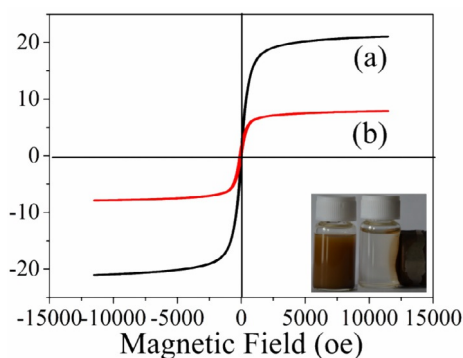


**Figure 4.** Room temperature magnetization curves of a)  $\text{Fe}_3\text{O}_4$  and b)  $\text{Fe}_3\text{O}_4\text{-L-dopa-Cu}^{\text{II}}/\text{Sn}^{\text{IV}}@m,m\text{-SiO}_2$ .

be seen that the magnetic saturation values of these are 21.0 and  $7.9 \text{ emu g}^{-1}$ , respectively. The decrease of the saturation magnetization suggests the presence of the mesoporous  $\text{SiO}_2$  shell and some  $\text{CuO}$  and  $\text{SnO}_2$  particles inside the uniformly pore of hollow mesoporous sphere.

### 3.2. Catalyst testing for B-V oxidation

The B-V oxidation of cyclohexanone was performed using air and various aldehyde over  $\text{Fe}_3\text{O}_4\text{-L-dopa-Cu}^{\text{II}}/\text{Sn}^{\text{IV}}@m,m\text{-SiO}_2$  in various solvent to find the optimum reaction conditions. Firstly, with cyclohexanone as the model substrate, the optimum reaction time, temperature, solvent, and the molar ratio of benzaldehyde/cyclohexanone were tested.

To investigate the effect of time on product distribution, reaction times of 1, 2, 3, 4, 5, 6, and 7 h were examined in the presence of the catalyst. The results of the influence of the reaction time on the exploration are presented in Figure 5. With increasing of the reaction time, the conversion of the reactants was increased as expected, while little change was observed after 6 h. The optimum reaction time was determined as 6 h.

Effects of the reaction temperature were shown in Figure 6. As we can see, with increasing the temperature, the conversion of cyclohexanone to  $\epsilon$ -caprolactone firstly increased but then reduced. At temperature from 303.15 to 343.15 K, the conversion of  $\epsilon$ -caprolactone firstly increased remarkably then decreased sharply. The optimized temperature was found at 323.15 K.

Presented in Table 1 is the influence of solvent on the B-V oxidation reaction of cyclohexanone over  $\text{Fe}_3\text{O}_4\text{-L-dopa-Cu}^{\text{II}}/\text{Sn}^{\text{IV}}@m,m\text{-SiO}_2$ .

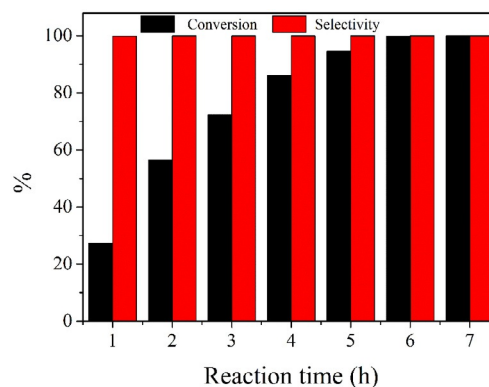


**Figure 5.** Effect of reaction time on the conversion of the B-V oxidation of cyclohexanone with  $\text{Fe}_3\text{O}_4\text{-L-dopa-Cu}^{\text{II}}/\text{Sn}^{\text{IV}}@m,m\text{-SiO}_2$  as catalyst. Reaction conditions: cyclohexanone (2 mmol), benzaldehyde (4 mmol), the catalyst (50 mg), 1,2-dichloroethane (10 mL), 323.15 K, air ( $20 \text{ mL min}^{-1}$ ). Legend: conversion (%). Determined by GC-MS measurement based on the internal standard method (dodecane).

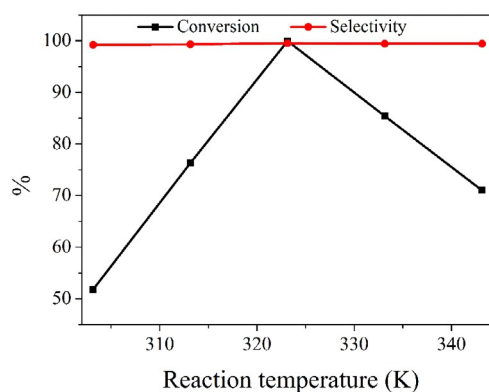


**Figure 6.** Effect of reaction temperature on the conversion of the B-V oxidation of cyclohexanone with  $\text{Fe}_3\text{O}_4\text{-L-dopa-Cu}^{\text{II}}/\text{Sn}^{\text{IV}}@m,m\text{-SiO}_2$  as catalyst. Reaction conditions: cyclohexanone (2 mmol), benzaldehyde (4 mmol), the catalyst (50 mg), 1,2-dichloroethane (10 mL), air ( $20 \text{ mL min}^{-1}$ ), 6 h. Legend: conversion (%). Determined by GC-MS measurement based on the internal standard method (dodecane).

**Table 1.** The effect of solvent on the conversion of the B-V oxidation of cyclohexanone with  $\text{Fe}_3\text{O}_4\text{-L-dopa-Cu}^{\text{II}}/\text{Sn}^{\text{IV}}@m,m\text{-SiO}_2$  as catalyst.<sup>[a]</sup>

Entry	Solvent	Conversion of cyclohexanone [%] <sup>[b]</sup>	Yield of $\epsilon$ -caprolactone [%] <sup>[b]</sup>	Selectivity of $\epsilon$ -caprolactone [%]
1	DCE	>99.9	>99.9	>99.9
2	water	82.5	82.5	>99.9
3	CHX	22.3	22.3	>99.9
4	AN	81.2	81.2	>99.9
5	DIOX	45.5	45.5	>99.9
6	DMSO	traces	traces	
7	THF	traces	traces	

[a] Reaction conditions: cyclohexanone (2 mmol), benzaldehyde (4 mmol), the catalyst (50 mg), solvent (10 mL), air ( $20 \text{ mL min}^{-1}$ ), 6 h, 323.15 K; [b] Conversion (%) is based on GC-MS analysis measurement based on the internal standard method (dodecane).

Sn<sup>IV</sup>@m-SiO<sub>2</sub>. It demonstrated that the solvent played an important role in the B-V oxidation system. The conversion of cyclohexanone was closely related with the polarity of solvent (Table 1, entries 1–4). The nonpolar solvent like 1,2-dichloroethane (DCE) was favorable to the oxidation of cyclohexanone, which gave higher conversion of cyclohexanone than that of polar solvent such as acetonitrile (AN) water and 1,4-dioxane (DIOX). Furthermore, the use of cyclohexane (CHX), *N,N*-dimethyl formamide (DMF) or tetrahydrofuran (THF) as solvent would result in poor performance. The water could also be used as solvent to the oxidation of cyclohexanone (Table 1, entry 2), but the conversion of cyclohexanone was lower than DCE. So the optimal solvent for cyclohexanone oxidation was DCE. In connection with the distinct results, it was supposed firstly that the solubility of in various solvents could be a possible reason. However, there was no substantial difference among them through our estimation. Therefore, the enhanced cyclohexanone conversion with nonpolar solvent is due to the solvation effect, rather than the Fe<sub>3</sub>O<sub>4</sub>-L-dopa-Cu<sup>II</sup>/Sn<sup>IV</sup>@m,m-SiO<sub>2</sub> catalyst solubility effect.

To investigate the effect of the molar ratio of benzaldehyde/cyclohexanone, the molar ratio of 1:1, 1.5:1, 2:1, 2.5:1, and 3:1 were examined in the presence of the catalyst. The effects of the molar ratio of benzaldehyde/cyclohexanone were shown in Table 2. It demonstrated that the molar ratio of benzaldehyde/cyclohexanone also played an important role.

**Table 2.** The effect of the molar ratio of benzaldehyde/cyclohexanone on the conversion of the B-V oxidation of cyclohexanone with Fe<sub>3</sub>O<sub>4</sub>-L-dopa-Cu<sup>II</sup>/Sn<sup>IV</sup>@m,m-SiO<sub>2</sub> as catalyst.<sup>[a]</sup>

Entry	Benzaldehyde/cyclohexanone [mmol mmol <sup>-1</sup> ]	Conversion of cyclohexanone [%]	Yield of ε-caprolactone [%]	Selectivity of ε-caprolactone [%]
1	1:1	75.2	75.2	> 99.9
2	1.5:1	98.1	98.1	> 99.9
3	2:1	> 99.9	> 99.9	> 99.9
4	2.5:1	> 99.9	> 99.9	> 99.9
5	3:1	> 99.9	> 99.9	> 99.9

[a] Reaction conditions: cyclohexanone 2 (mmol), the catalyst (50 mg), DCE (10 mL), air (20 mL min<sup>-1</sup>), 6 h, 323.15 K; [b] Conversion (%) is based on GC-MS analysis measurement based on the internal standard method (dodecane).

The result of the B-V oxidation of cyclohexanone with various aldehyde as sacrificing agents are summarized in Table 3. It can be seen clearly that 1) benzaldehyde was favorable to the oxidation of cyclohexanone, which gave higher conversion of cyclohexanone than 4-bromine benzaldehyde and *p*-tolualdehyde. 2) The effect of substituent in various benzaldehyde also influenced the conversion of cyclohexanone in B-V oxidation (Table 3, entries 2–4). The benzaldehydes with an electron-withdrawing group can perform as a better sacrificing agents than the benzaldehydes with electron donating group for B-V oxidation (Table 3, entries 2–4). The benzaldehydes with an electron-withdrawing group or an electron donating group perform worse than the benzaldehyde (Table 3, entries 2–4, 1). 3) Furthermore, most aromatic aldehydes perform better than fatty aldehydes (Table 3, entries 1–3, 5–7). Therefore, aldehydes played an important role in the B-V oxidation system. It was supposed that the mechanism of the B-V oxidation involved free radical species.

The present oxidation system could be attractive if it can be applied to various ketones. To evaluate the scope of catalytic system, the catalytic activities towards B-V oxidation of various ketones were also explored and the results were shown in Table 4. Cyclohexanone and cyclopentanone are more easily than other ketones to convert into corresponding ester, which was consistent with results of other reports,<sup>[2,3]</sup> and *p*-methylacetophenone is more easily than acetophenone to convert into corresponding ester. Because methyl is a group which is able to stabilize the positive charge.<sup>[16]</sup> The fatty ketones is difficult to transform into corresponding ester through B-V oxidation reaction.

Table 5 showed the comparative analysis of catalytic activity of Fe<sub>3</sub>O<sub>4</sub>-L-dopa-Cu<sup>II</sup>/Sn<sup>IV</sup>@m,m-SiO<sub>2</sub> catalyst with other reported solid catalysts for B-V oxidation of cyclohexanone to ε-caprolactone in O<sub>2</sub>/benzaldehyde system. It clearly exhibited that the Fe<sub>3</sub>O<sub>4</sub>-L-dopa-Cu<sup>II</sup>/Sn<sup>IV</sup>@m,m-SiO<sub>2</sub> catalyst performed better catalytic activity over the reported catalytic systems: Graphite, FeTPPCI/SnO<sub>2</sub>, Ketjen Black and MnALPO-36 with respect to the yield of ε-caprolactone. The other reported catalytic systems suffered from the limitations of relatively low activity, higher amounts of benzaldehyde or longer reaction time. Though the reaction time of graphite catalytic system is shorter and the amounts of benzaldehyde (benzaldehyde/cyclohex-

**Table 3.** The effect of various aldehyde on the conversion of the B-V oxidation of cyclohexanone with Fe<sub>3</sub>O<sub>4</sub>-L-dopa-Cu<sup>II</sup>/Sn<sup>IV</sup>@m,m-SiO<sub>2</sub> as catalyst.<sup>[a]</sup>

Entry	Aldehyde	Aldehyde/cyclohexanone [mmol mmol <sup>-1</sup> ] <sup>[b]</sup>	Conversion of cyclohexanone [%] <sup>[b]</sup>	Yield of ε-caprolactone [%]	Selectivity of ε-caprolactone [%]
1	benzaldehyde	2:1	> 99.9	> 99.9	> 99.9
2	4-bromine benzaldehyde	2:1	74.0	74.0	> 99.9
3	<i>p</i> -tolualdehyde	2:1	63.3	63.3	> 99.9
4	<i>p</i> -anisaldehyde	2:1	14.7	14.7	> 99.9
5	isobutyraldehyde	2:1	36.4	36.4	> 99.9
6	aldehyde	2:1	3.3	3.3	> 99.9
7	methanal <sup>[b]</sup>	2:1	0.1	0.1	> 99.9

[a] Reaction conditions: cyclohexanone 2 mmol, aldehyde 4 mmol, the catalyst 50 mg, 1, DCE 10 mL, air 20 mL min<sup>-1</sup>, 6 h, 323.15 K; [b] Conversion (%) is based on GC-MS measurement based on the internal standard method (dodecane).

Entry	Substrate	Product	Conversion [%] <sup>[b]</sup>	Yield [%] <sup>[b]</sup>	Selectivity [%]
1			> 99.9	> 99.9	> 99.9
2			68.9	68.9	> 99.9
3			0.1	0.1	> 99.9
4			60.8	60.8	> 99.9
5			traces		

[a] Reaction conditions: ketones 2 mmol, aldehyde 4 mmol, the catalyst 50 mg, DEC 10 mL, air 20 mL min<sup>-1</sup>, 6 h, 323.15 K; [b] Conversion (%) is based on GC-MS.

anone = 1:1) of the Ketjen Black catalytic system is lower than the Fe<sub>3</sub>O<sub>4</sub>-L-dopa-Cu<sup>II</sup>/Sn<sup>IV</sup>@m,m-SiO<sub>2</sub> catalyst catalytic system, they suffered from the same limitations of relatively low activity.

The Fe<sub>3</sub>O<sub>4</sub>-L-dopa-Cu<sup>II</sup>/Sn<sup>IV</sup>@m,m-SiO<sub>2</sub> catalyst could be easily separated by using an external magnet and reused after being calcined in air at 500 °C for 6 h. Figure 7 shows the performance of Fe<sub>3</sub>O<sub>4</sub>-L-dopa-Cu<sup>II</sup>/Sn<sup>IV</sup>@m-SiO<sub>2</sub> in cycles of cyclohexanone oxidation at 323.15 K in 6 h. It is clear that the Fe<sub>3</sub>O<sub>4</sub>-L-dopa-Cu<sup>II</sup>/Sn<sup>IV</sup>@m,m-SiO<sub>2</sub> catalyst shows steady performance across the five runs, indicating that Fe<sub>3</sub>O<sub>4</sub>-L-dopa-Cu<sup>II</sup>/Sn<sup>IV</sup>@m,m-SiO<sub>2</sub> is a stable catalyst reusable for the B-V oxidation reaction.

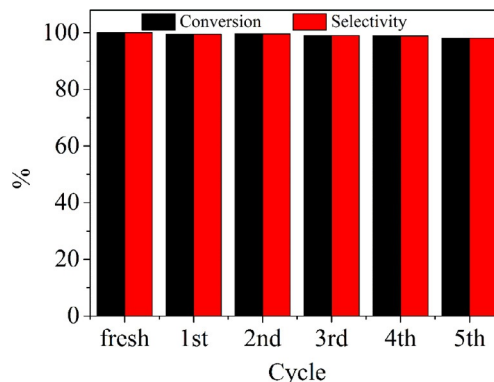


**Figure 7.** Reuse of Fe<sub>3</sub>O<sub>4</sub>-L-dopa-Cu<sup>II</sup>/Sn<sup>IV</sup>@m,m-SiO<sub>2</sub> for the BV oxidation using air and benzaldehyde. Reaction conditions: cyclohexanone (2 mmol), benzaldehyde (4 mmol), the catalyst (50 mg), 1,2-dichloroethane (10 mL), 323.15 K, 6 h, air (20 mL min<sup>-1</sup>). Legend: conversion (%). Determined by GC-MS measurement based on the internal standard method (dodecane).

### 3.3. Plausible mechanism for the cocatalytic cyclohexanone oxidation

The catalysis of Fe<sub>3</sub>O<sub>4</sub>-L-dopa-Sn<sup>IV</sup>@m,m-SiO<sub>2</sub>, Fe<sub>3</sub>O<sub>4</sub>-L-dopa-Cu<sup>II</sup>@m,m-SiO<sub>2</sub>, and Fe<sub>3</sub>O<sub>4</sub>-L-dopa-Cu<sup>II</sup>/Sn<sup>IV</sup>@m,m-SiO<sub>2</sub> for the Baeyer–Villiger type oxidation were examined by performing the oxidation of cyclohexanone to ε-caprolactone in the presence of benzaldehyde. Table 6 summarizes the results of the cyclohexanone oxidation under air atmosphere at 50 °C. The three kinds of catalysts showed high selectivity, over 99.9%, and Fe<sub>3</sub>O<sub>4</sub>-L-dopa-Cu<sup>II</sup>/Sn<sup>IV</sup>@m,m-SiO<sub>2</sub> showed the highest conversion, over 99.9%, under this experimental condition. Whereas the blank run without catalyst resulted in quite poor conversion, just 16.0%. It indicated that catalyst played an important role for the cyclohexanone oxidation. In addition, in the Fe<sub>3</sub>O<sub>4</sub>-L-dopa-Cu<sup>II</sup>@m,m-SiO<sub>2</sub> or Fe<sub>3</sub>O<sub>4</sub>-L-dopa-Cu<sup>II</sup>/Sn<sup>IV</sup>@m,m-SiO<sub>2</sub> system, there was formic acid phenyl ester which was the by-product of benzaldehyde, and both the generation rate of formic acid phenyl ester were about 10%. However, in the Fe<sub>3</sub>O<sub>4</sub>-L-dopa-Sn<sup>IV</sup>@m,m-SiO<sub>2</sub> or no catalyst system, there was no formic acid phenyl ester. It was proposed that Cu<sup>II</sup> as Lewis acid might activate benzaldehyde which could improve the generation rate of peroxybenzoic acid. When the concentration

Entry	Catalysts	t [h]	Conversion of cyclohexanone [%] <sup>[b]</sup>	Yield of ε-caprolactone [%] <sup>[b]</sup>	Selectivity of ε-caprolactone [%] <sup>[b]</sup>	Ref.
1	Fe <sub>3</sub> O <sub>4</sub> -L-dopa-Cu <sup>II</sup> /Sn <sup>IV</sup> @m,m-SiO <sub>2</sub>	3	> 99.9	> 99.9	> 99.9	this work
2	Fe <sub>3</sub> O <sub>4</sub> -L-dopa-Cu <sup>II</sup> /Sn <sup>IV</sup> @m,m-SiO <sub>2</sub>	6	> 99.9	> 99.9	> 99.9	this work
3	Ketjen Black <sup>[e]</sup>	6	91.0	91.0	> 99.0	[1]
4	FeTPPCI/SnO <sub>2</sub>	8	96.0	96.0	> 99.0	[2]
5	Graphite <sup>[d]</sup>	3	99.6	99.0	99.4	[3]
6	MnALPO-36 <sup>[f]</sup>	6	78.0	76.4	98.0	[27]

[a] Reaction conditions: cyclohexanone (2 mmol), benzaldehyde (4 mmol), the catalyst (50 mg), DEC (10 mL), 323.15 K; [b] Conversion (%) is based on GC-MS; [c] Using air and benzaldehyde as oxidant; [d] Cyclohexanone (4 mmol), benzaldehyde (4 mmol); [e] Cyclohexanone (10 mmol), benzaldehyde (20 mmol), DEC (20 mL); [f] Cyclohexanone/benzaldehyde = 1:3 (mol: mol).

**Table 6.** The results of the cyclohexanone oxidation catalyzed by Fe<sub>3</sub>O<sub>4</sub>-L-dopa-Sn<sup>IV</sup>@m,m-SiO<sub>2</sub>, Fe<sub>3</sub>O<sub>4</sub>-L-dopa-Cu<sup>II</sup>@m,m-SiO<sub>2</sub> and Fe<sub>3</sub>O<sub>4</sub>-L-dopa-Cu<sup>II</sup>/Sn<sup>IV</sup>@m,m-SiO<sub>2</sub> under air atmosphere at 50 °C.<sup>[a]</sup>

Entry	Catalysts	t [h]	Yield of ε-caprolactone [%] <sup>[b]</sup>	Yield of formic acid phenyl ester [%] <sup>[b]</sup>
1	Fe <sub>3</sub> O <sub>4</sub> -L-dopa-Sn <sup>IV</sup> @m,m-SiO <sub>2</sub>	6	32.8	traces
2	Fe <sub>3</sub> O <sub>4</sub> -L-dopa-Cu <sup>II</sup> @m,m-SiO <sub>2</sub>	6	81.8	10.9
3	Fe <sub>3</sub> O <sub>4</sub> -L-dopa-Cu <sup>II</sup> /Sn <sup>IV</sup> @m,m-SiO <sub>2</sub>	6	> 99.9	11.3
4	none	6	16.0	traces

[a] Reaction conditions: cyclohexanone (2 mmol), benzaldehyde (4 mmol), the catalyst (50 mg), DEC (10 mL), 323.15 K; [b] Conversion (%) is based on GC-MS.

of peroxybenzoic acid reaches a certain value, benzaldehyde could be oxidized into formic acid phenyl ester. Nevertheless, Sn<sup>IV</sup> could not or weakly activate benzaldehyde. The mechanism involved free radical species was identified in the oxidation of cyclohexanone by adding radical trap (BHT, 2,6-di-tert-butyl-4-methylphenol), and the reaction was totally inhibited and that the mechanism involved radical could be identified the experimental results (Table 3, entries 2–4).

In the mechanism, the reaction efficiency is usually related with the generation rate of peroxybenzoic acid and Criegee adduct-like intermediate. As previous research has shown, SnO<sub>2</sub> can be used as a Lewis acid catalyst owing to its acid site.<sup>[28–31]</sup> Carbonyl compounds could be activated by the coordination between the oxygen atom of the carbonyl group and the Lewis acid site. For the bimetallic catalyst oxidation system, the generation rate of peroxybenzoic acid could be improved if there is the coordination between benzaldehyde and Lewis acid site. On the other hand, the formation rate of Criegee adduct-like intermediate should be accelerated in the presence of the coordination between cyclohexanone and SnO<sub>2</sub> and Cu<sup>II</sup>.

To obtain further insights into the role of SnO<sub>2</sub> and CuO in the observed acceleration, the following experiments were conducted. Firstly, the catalysis of Fe<sub>3</sub>O<sub>4</sub>-L-dopa-Sn<sup>IV</sup>@m,m-SiO<sub>2</sub>, Fe<sub>3</sub>O<sub>4</sub>-L-dopa-Cu<sup>II</sup>@m,m-SiO<sub>2</sub>, and Fe<sub>3</sub>O<sub>4</sub>-L-dopa-Cu<sup>II</sup>/Sn<sup>IV</sup>@m,m-SiO<sub>2</sub> for the oxidation of benzaldehyde (Table 7). In the Fe<sub>3</sub>O<sub>4</sub>-L-dopa-Sn<sup>IV</sup>@m-SiO<sub>2</sub> system, moderate yield of benzoic acid could be obtained by conducting the reaction for 6 h and there was no formic acid phenyl ester. Whereas, in the Fe<sub>3</sub>O<sub>4</sub>-L-

**Table 7.** Further insights into the role of SnO<sub>2</sub> and CuO for the oxidation of benzaldehyde.<sup>[a]</sup>

Entry	Catalysts	t [h]	Yield of benzoic acid [%] <sup>[b]</sup>	Yield of formic acid phenyl ester [%] <sup>[b]</sup>
1	Fe <sub>3</sub> O <sub>4</sub> -L-dopa-Sn <sup>IV</sup> @m-SiO <sub>2</sub>	6	32.8	traces
2	Fe <sub>3</sub> O <sub>4</sub> -L-dopa-Cu <sup>II</sup> @m-SiO <sub>2</sub>	6	81.8	10.9
3	Fe <sub>3</sub> O <sub>4</sub> -L-dopa-Cu <sup>II</sup> /Sn <sup>IV</sup> @m-SiO <sub>2</sub>	6	86.5	11.3

[a] Reaction conditions: 4 mmol benzaldehyde, the catalyst 50 mg, DEC 10 mL, 323.15 K; [b] Conversion (%) is based on GC-MS.

dopa-Cu<sup>II</sup>@m-SiO<sub>2</sub>, or Fe<sub>3</sub>O<sub>4</sub>-L-dopa-Cu<sup>II</sup>/Sn<sup>IV</sup>@m,m-SiO<sub>2</sub> system the reaction rate was accelerated remarkably and over 80% benzaldehyde could be converted to benzoic acid and about 10% benzaldehyde was converted to formic acid phenyl ester. These results could further prove that Cu<sup>II</sup> could be used as Lewis acid to activate benzaldehyde and Sn<sup>IV</sup> as Lewis acid could weakly activate benzaldehyde. Secondly, the B-V oxidation reaction of cyclohexanone was conducted by various catalysts with metachloroperbenzoic acid as oxidant. The results were summarized in Table 8. In the system of no catalyst, moderate yield of ε-caprolactone could be obtained by conducting

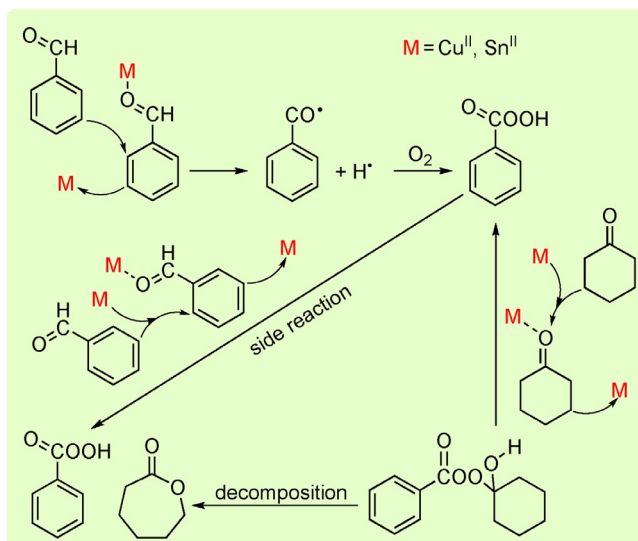
**Table 8.** Further insights into the role of SnO<sub>2</sub> and CuO for the oxidation of cyclohexanone.<sup>[a]</sup>

Entry	Catalysts	t [h]	Yield of ε-caprolactone [%] <sup>[b]</sup>
1	no catalyst	0.5	35.5
2	Fe <sub>3</sub> O <sub>4</sub> -L-dopa-Sn <sup>IV</sup> @m-SiO <sub>2</sub>	0.5	84.3
3	Fe <sub>3</sub> O <sub>4</sub> -L-dopa-Cu <sup>II</sup> @m-SiO <sub>2</sub>	0.5	41.3

[a] Reaction conditions: 4 mmol benzaldehyde, the catalyst 50 mg, DEC 10 mL, 323.15 K; [b] Conversion (%) is based on GC-MS.

the reaction for 2 h. In the Fe<sub>3</sub>O<sub>4</sub>-L-dopa-Sn<sup>IV</sup>@m,m-SiO<sub>2</sub> or Fe<sub>3</sub>O<sub>4</sub>-L-dopa-Cu<sup>II</sup>@m,m-SiO<sub>2</sub> system, the conversion of cyclohexanone was higher, and the yield of ε-caprolactone could be reached to 92.1% only for 0.5 h. The above results proved that both Sn<sup>IV</sup> and Cu<sup>II</sup> could activate cyclohexanone and the former showed better activation capacity than the latter to cyclohexanone. Thirdly, the oxidation of benzaldehyde was conducted by Fe<sub>3</sub>O<sub>4</sub>-L-dopa-Cu<sup>II</sup>/Sn<sup>IV</sup>@m,m-SiO<sub>2</sub> catalyst with metachloroperbenzoic acid as oxidant. The yield of benzoic acid and formic acid phenyl ester were 60.0 and 28.0, respectively by conducting the reaction for 2 h, which proved benzaldehyde could be oxidized into formic acid phenyl ester.

Based on the discussion above, the catalytic mechanism of Fe<sub>3</sub>O<sub>4</sub>-L-dopa-Cu<sup>II</sup>/Sn<sup>IV</sup>@m,m-SiO<sub>2</sub> for the oxidation of cyclohexanone was proposed as shown in Scheme 2. In the catalytic mechanism, Cu<sup>II</sup> played important roles that could activate benzaldehyde and cyclohexanone molecules in the aerobic oxidation of cyclohexanone, but the former was the main role. Sn<sup>IV</sup> mainly activates cyclohexanone molecules in the aerobic oxidation of cyclohexanone. The Lewis acid sites (Sn<sup>IV</sup> and Cu<sup>II</sup>) coordinated with the oxygen atom of the carbonyl group, which activated the cyclohexanone molecules in the reaction. An easier nucleophilic attack of organic peracids on the activated cyclohexanone favored the formation of a Criegee adduct, followed by rearrangement to form ε-caprolactone.



**Scheme 2.** Possible reaction pathway involved in the B-V oxidation of cyclohexanone.

## Conclusions

In conclusion, we describe a method to form  $\text{Fe}_3\text{O}_4\text{-L-dopa-Cu}^{\text{II}}/\text{Sn}^{\text{IV}}@m,m\text{-SiO}_2$  catalyst, and the catalyst shows high performance for synthesis of  $\epsilon$ -caprolactone through B-V oxidation reaction. The system of  $\text{Fe}_3\text{O}_4\text{-L-dopa-Cu}^{\text{II}}/\text{Sn}^{\text{IV}}@m,m\text{-SiO}_2$  bi-metallic catalyst promoted the formation of  $\epsilon$ -caprolactone. In the catalytic mechanism,  $\text{Cu}^{\text{II}}$  as Lewis acid played an important role that could activate benzaldehyde and cyclohexanone molecules in the aerobic oxidation of cyclohexanone, however, the former was dominating.  $\text{Sn}^{\text{IV}}$  as Lewis acid, however, could mainly activate cyclohexanone. Moreover,  $\text{Fe}_3\text{O}_4\text{-L-dopa-Cu}^{\text{II}}/\text{Sn}^{\text{IV}}@m,m\text{-SiO}_2$  catalyst could be easily separated by an external magnet. The catalyst showed stable catalytic activity for the B-V oxidation reaction and could be reused without any notable loss in catalytic activity at least up to five cycles.

## Acknowledgements

This work was supported by the Key Projects in the National Science and Technology Pillar Program of China (2014 4BAK16B01) and the Fundamental Research Funds for the Central Universities (lzujbky-2015-16 and lzujbky-2015-17).

**Keywords:** Baeyer–Villiger • copper • oxidation • tin

- [1] Y. Nabae, H. Rokubuichi, M. Mikuni, Y. Kuang, T. Hayakawa, M.-a. Kakimoto, *ACS Catal.* **2013**, *3*, 230–236.
- [2] S. Chen, X. Zhou, Y. Li, R. Luo, H. Ji, *Chem. Eng. J.* **2014**, *241*, 138–144.
- [3] Y.-F. Li, M.-Q. Guo, S.-F. Yin, L. Chen, Y.-B. Zhou, R.-H. Qiu, C.-T. Au, *Carbon* **2013**, *55*, 269–275.
- [4] R. Strukul, *Angew. Chem. Int. Ed.* **1998**, *37*, 1198–1209; *Angew. Chem.* **1998**, *110*, 1256–1267.
- [5] G.-J. ten Brink, I. W. C. E. Arends, R. A. Sheldon, *Chem. Rev.* **2004**, *104*, 4105–4123.
- [6] R. A. Michelin, P. Sgarbossa, A. Scarso, G. Strukul, *Coord. Chem. Rev.* **2010**, *254*, 646–660.
- [7] A. Sinhamahapatra, A. Sinha, S. K. Pahari, N. Sutradhar, H. C. Bajaj, A. B. Panda, *Catal. Sci. Technol.* **2012**, *2*, 2375–2382.
- [8] T. Hara, M. Hatakeyama, A. Kim, N. Ichikuni, S. Shimazu, *Green Chem.* **2012**, *14*, 771–777.
- [9] C. Chen, J. Peng, B. Li, L. Wang, *Catal. Lett.* **2009**, *131*, 618–623.
- [10] S. Kirumakki, S. Samarajeewa, R. Harwell, A. Mukherjee, R. H. Herber, A. Clearfield, *Chem. Commun.* **2008**, 5556–5558.
- [11] A. Cavarzan, A. Scarso, P. Sgarbossa, R. A. Michelin, G. Strukul, *ChemCatChem* **2010**, *2*, 1296–1302.
- [12] C. Jiménez-Sanchidrián, J. R. Ruiz, *Tetrahedron* **2008**, *64*, 2011–2026.
- [13] T. Yamada, T. Takai, O. R. and, T. Mukaiyama, *Chem. Lett.* **1991**, 1–4.
- [14] R. Mello, A. Olmos, J. Parra-Carbonell, M. E. González-Núñez, G. Asensio, *Green Chem.* **2009**, *11*, 994–999.
- [15] R. Llamas, C. Jiménez-Sanchidrián, J. R. Ruiz, *Appl. Catal. B* **2007**, *72*, 18–25.
- [16] A. Corma, L. T. Nemeth, M. Renz, S. Valencia, *Nature* **2001**, *412*, 423–425.
- [17] M. Renz, T. Blasco, A. Corma, V. Fornes, R. Jensen, L. Nemeth, *Chem. Eur. J.* **2002**, *8*, 4708–4717.
- [18] A. Corma, M. a. T. Navarro, M. Renz, *J. Catal.* **2003**, *219*, 242–246.
- [19] S. E. Allen, R. R. Walvoord, R. Padilla-Salinas, M. C. Kozłowski, *Chem. Rev.* **2013**, *113*, 6234–6458.
- [20] A. E. Wendlandt, A. M. Suess, S. S. Stahl, *Angew. Chem. Int. Ed.* **2011**, *50*, 11062–11087; *Angew. Chem.* **2011**, *123*, 11256–11283.
- [21] X. Su, D. J. Fox, D. T. Blackwell, K. Tanaka, D. R. Spring, *Chem. Commun.* **2006**, 3883–3885.
- [22] M. T. Wentzel, J. B. Hewgley, R. M. Kamble, P. D. Wall, M. C. Kozłowski, *Adv. Synth. Catal.* **2009**, *351*, 931–937.
- [23] J. B. Lan, L. Chen, X. Q. Yu, J. S. You, R. G. Xie, *Chem. Commun.* **2004**, 188–189.
- [24] M. Enomoto, S. Kuwahara, *Angew. Chem. Int. Ed.* **2009**, *48*, 1144–1148; *Angew. Chem.* **2009**, *121*, 1164–1168.
- [25] Y. Bolshan, R. A. Batey, *Angew. Chem. Int. Ed.* **2008**, *47*, 2109–2112; *Angew. Chem.* **2008**, *120*, 2139–2142.
- [26] H. Zhu, C. Hou, Y. Li, G. Zhao, X. Liu, K. Hou, Y. Li, *Chem. Asian J.* **2013**, *8*, 1447–1454.
- [27] R. Raja, J. M. Thomas, a. G. Sankar, *Chem. Commun.* **1999**, 525–526.
- [28] Y. Murakami, K. Iwayama, H. Uchida, T. Hattori, T. Tagawa, *J. Catal.* **1981**, *71*, 257–269.
- [29] H. Yagita, K. Asami, A. Muramatsu, K. Fujimoto, *Appl. Catal.* **1989**, *53*, L5L9.
- [30] H. Wang, Y. Wang, J. Xu, H. H. Yang, C. S. Lee, A. L. Rogach, *Langmuir* **2012**, *28*, 10597–10601.
- [31] X. Wang, X. Han, S. Xie, Q. Kuang, Y. Jiang, S. Zhang, X. Mu, G. Chen, Z. Xie, L. Zheng, *Chem. Eur. J.* **2012**, *18*, 2283–2289.

Received: October 9, 2015

Revised: October 25, 2015

Published online on January 15, 2016